Hydrogen-Bonded Multilayers for the Release of Polyelectrolyte Nanotubes in Biocompatible Conditions

Wanlin Xu, Etienne Ferain, Sophie Demoustier-Champagne,

Karine Glinel and Alain M. Jonas

Institute of Condensed Matter and Nanosciences, Université catholique de Louvain, Croix du Sud 1 L7.04.02, 1348 Louvain-la-Neuve, Belgium.

TOC

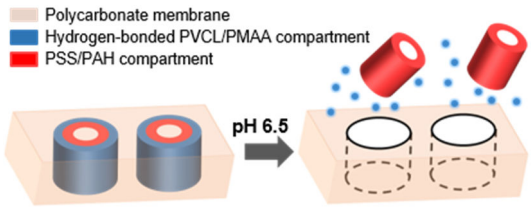

Abstract

The growth and disaggregation of hydrogen-bonded layer-by-layer (LbL) multilayers based on poly(methacrylic acid) (PMAA) and poly(*N*-vinyl caprolactam) (PVCL) are studied depending on pH, NaCl concentration and PVCL molar mass. Whereas multilayer growth is essentially insensitive to salt and PVCL molar mass, the critical pH for disaggregation strongly depends on salt concentration. The PMAA/PVCL multilayers are then used as sacrificial compartments for the release of LbL nanostructures in biocompatible close-to-neutral 0.15 M NaCl aqueous conditions. We particularly demonstrate the liberation of LbL nanotubes grown inside the nanopores of templating polymer membranes without having to dissolve the membrane template

in non-biocompatible organic solvents, and show that the amount of released nanotubes is close to the amount of non-crossing nanopores in the membrane.

Introduction

Layer-by-layer (LbL) assembly is an efficient methodology to create functional coatings on a variety of substrates.[1-11] When performing LbL inside the pores of a nanoporous membrane, LbL assembly provides access to in-template nanostructures replicating the porosity of the membrane.[12-16] Dissolution of the membrane then leads to free nanostructures of cylindrical shape, *i.e.*, nanotubes (NTs)[17] and nanowires (Scheme 1a),[18] which can be used for a variety of applications. Among these, biological applications such as delivery carriers,[19-22] porous enzymatic nanotube mats,[23-26] or bacterial patches[27] have been proposed. For applications that involve sensitive biomacromolecules or living organisms, the dissolution step of the templating membrane is a significant issue, as it often occurs in conditions that may denature or kill the biological components.

For instance, when using nanoporous track-etched polycarbonate (PC) membranes as templates, the dissolution step is typically done in an organic solvent such as dichloromethane,[28] which is especially adverse for biological applications and creates safety issues (Scheme 1a). Here, we propose and study an alternative methodology of NT liberation, based on the fabrication in the nanopores of PC membranes of bi-compartmentalized NTs having a sacrificial outer compartment that can be erased to liberate the inner NT compartment in biologically-compatible conditions (Scheme 1b). The erasable compartment is stable up to pH 6 in 0.15 M NaCl aqueous solution and can be erased at a slightly higher, close to neutral pH. These conditions are compatible

with the inclusion of living organisms such as viruses or bacteria in the templated tubes and fully eliminates the need to use organic solvents for tube recovery.

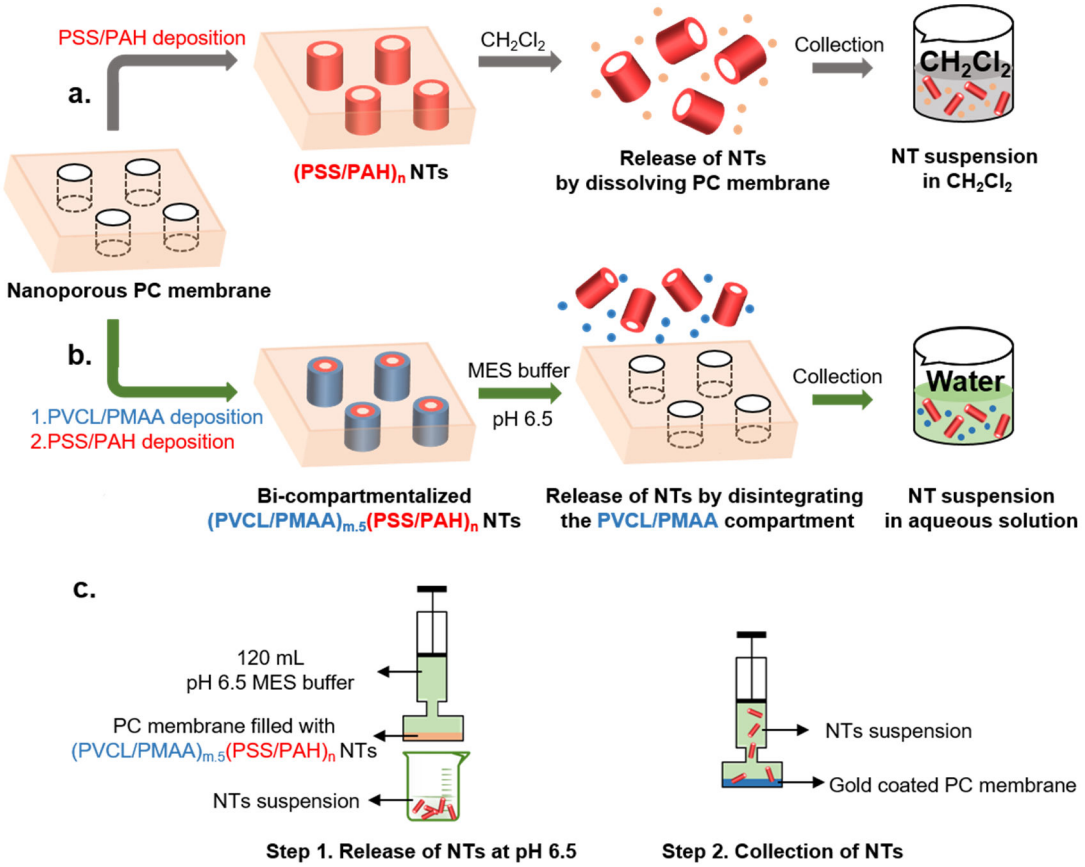

Scheme 1. (a) Scheme of the standard LbL process of NT fabrication in the pores of a membrane, requiring the dissolution of the templating membrane in non-biocompatible solvents to recover the NTs. (b) Schematic illustration of the fabrication of bi-compartmentalized $(PVCL/PMAA)_{m.5}(PSS/PAH)_n$ NTs, and of the release of the inner NTs in biologically-compatible conditions. (c) The release and collection of the inner $(PSS/PAH)_n$ NT compartments is performed by disaggregating the sacrificial outer $(PVCL/PMAA)_{m.5}$ compartment in a pH 6.5 aqueous solution while pushing the inner compartments outside the pores of the membrane.

Previous work on erasable LbL compartments focused on hydrogen-bonded (H-bonded) flat multilayers, providing a good starting point for the development of a water-based liberation method of NTs.[29-35] Such systems can be grown at pH values for which the H-bond-donating polymeric component is protonated; at higher pH, the degree of ionization of this component is increased, resulting in a weakening of its H-bond-donating capability with a simultaneous increase of electrostatic repulsions, leading to the disaggregation of the multilayers. Different systems are characterized by different values of critical pH at which the multilayer starts to become unstable. In particular, Sukhishvili *et al.* extensively studied H-bonded LbL systems with critical pHs ranging from 3.3 to 9.5. For instance, poly(acrylic acid)/poly(ethylene oxide) (PAA/PEO) multilayers have a low critical pH of 3.3 because of the weak H-bonds established between PAA and PEO.[36] The use of polyacids of higher pKa value, for example poly(methacrylic acid) (PMAA, pKa *ca.* 4.5) and poly(ethacrylic acid) PEAA (pKa *ca.* 7), and/or of more hydrophobic neutral polymers such as poly(*N*-isopropyl acrylamide) (PNIPAAm), results in an increase of the critical pH of multilayers to *ca.* 6.0.[37] These authors also succeeded in reaching even higher critical pH values (8.0-9.5) by depositing tannic acid (TA), whose pKa is *ca.* 8.5, with several neutral H-bond accepting polymers.[38]

We therefore screened the literature, aiming at identifying the most promising system for biocompatible release of LbL NTs, *i.e.*, a system that would be stable in 150 mM NaCl solution at *ca.* pH 6 and would dissolve at *ca.* pH 7, which would be optimal for biological applications. No system was exactly fitting these requirements; nevertheless, we identified (PMAA/poly(*N*-vinyl caprolactam) (PVCL)) systems as promising (Scheme 2), since they were reported to disintegrate at pH 6.5 in 10 mM phosphate buffer.[37]

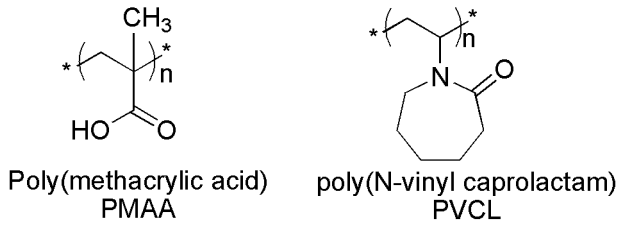

Scheme 2. Chemical structure of the H-bonding polymers of this study.

Additionally, the effect on multilayer stability of a biological concentration of NaCl was rarely considered in the literature. Previous work on polyphenol/neutral polymer systems such as TA/PEO, TA/PNIPAAm, and TA/PVPON showed that the critical pH for film disintegration decreases by 0.5 pH units in 150 mM NaCl for these systems.[38] A similar phenomenon is to be expected for PMAA/PVCL, but was not studied so far. Therefore, in this article, we focus on the growth and disintegration of PMAA/PVCL LbL multilayers depending on pH, NaCl concentration and PVCL molar mass, parameters which have not been studied in depth before. We then use PMAA/PVCL multilayers to build sacrificial compartments below flat LbL films and as external compartments in templated LbL NTs, and demonstrate the floating-off of flat films and the release of NTs in biocompatible conditions.

Experimental section

Materials. Poly(methacrylic acid) (PMAA, M_w 100 kg/mol) was obtained from Polysciences, and poly(N-vinyl caprolactam)s (PVCL, M_w 1.8, 32 and 240 kg/mol) were purchased from Polymer Source Inc. Poly(vinyl pyrrolidone) (PVPON, M_w 1 300 kg/mol), branched polyethylenimine (bPEI, M_w 750 kg/mol), 2-(*N*-morpholino)ethanesulfonic acid (MES) and sodium alginate (ALG) were purchased

from Sigma-Aldrich. Poly(styrenesulfonate) (PSS, M_w 70 kg/mol), and NaCl (ACS reagent) were obtained from Acros. Poly(allylamine hydrochloride) (PAH, M_w 120-200 kg/mol) was obtained from Alfa Aesar. Rhodamine-labeled PAH (PAH-Rh, M_w 15 kg/mol, 1:392 mol:mol monomer ratio in dye) was purchased from Surflay Nanotec GmbH. Chitosan (CHI, M_w 50-150 kg/mol, deacetylation degree > 90%) was from NovaMatrix.

Polymer solutions of varying NaCl concentration were prepared at 1 mg/mL except for PAH-Rh (0.5 mg/mL) and bPEI (0.5 mg/mL). Track-etched polycarbonate membranes (PC membranes of 800 nm pore diameter, 24 μm thickness, with either 4×10^7 pores cm^{-2} or 1×10^7 pores cm^{-2}) and polyethylene terephthalate membranes (PET membranes) were provided by it4ip (Belgium) and used as received. Silicon wafers obtained from Topsil Germany were cleaned in acetone then isopropanol and MilliQ water, and treated by air plasma (ETMITECH K1050X) before LbL deposition. MilliQ water with a resistivity of 18.2 MΩ.cm was obtained from a Merck Millipore system and used in all experiments.

Fabrication of flat LbL films (PMAA/PVCL, PMAA/PVPON, PSS/PAH, ALG/CHI). PMAA/PVCL and PMAA/PVPON multilayers were deposited at pH 2.0, conditions in which PMAA is fully protonated, on Si wafers. To enhance polymer adsorption, a precursor layer was first deposited by dipping clean Si wafers in a bPEI solution (pH 2.0; 0, 50 or 150 mM in NaCl) for 10 min followed by triple rinsing in solutions of same pH and NaCl concentration as the bPEI solution (30 s each). Si wafers were then alternately immersed in PMAA and PVCL solutions for 5 min. Between each adsorption, Si wafers were rinsed three times (30 s each).

PSS/PAH deposition was carried out at pH 4.0 using a similar procedure as above, and 0.5 mg/mL PAH-Rh was used to label the films in the last five cycles. PSS/PAH

multilayers were either directly deposited on Si wafers (with a precursor bPEI layer), leading to PEI/$(PSS/PAH)_n$ films, or deposited on top of PEI/$(PMAA/PVCL)_m$ films to obtain bi-compartmentalized PEI/$(PMAA/PVCL)_m$/$(PSS/PAH)_n$ films. The same procedure as for PSS/PAH was followed for ALG/CHI deposition at pH 4.0, leading to PEI/$(ALG/CHI)_n$ films and PEI/$(PMAA/PVCL)_m$/$(ALG/CHI)_n$ films. For all LbL assemblies, no intermediate drying was performed until the desired number of bilayers was obtained, after which coated Si wafers were rinsed with MilliQ water (3 s), then carefully dried with a stream of nitrogen for thickness measurement.

Fabrication of bi-compartmentalized LbL NTs

Track-etched PC membranes were used as received to prepare core-shell NTs comprising a PVCL/$(PMAA/PVCL)_m$ external compartment (hereafter noted $(PVCL/PMAA)_{m.5}$) and a $(PSS/PAH)_n$ inner compartment (Scheme 1b), deposited at pH 2.0 and 4.0, respectively; the NaCl concentration was fixed at 150 mM for all steps. A 4×10^7 pores cm^{-2} PC membrane was used to prepare the NTs unless otherwise indicated. Since most material surfaces are negatively-charged in water unless the pH is low, the deposition of the second compartment always started with the negatively-charged PSS to decrease the trend of liberated $(PSS/PAH)_n$ NTs to stick on solid surfaces after dissolution of the sacrificial PVCL/PMAA compartment. Therefore, the deposition of the external PVCL/PMAA compartment always started and ended with PVCL. A 6×6 cm^2 membrane was dipped in polymer solutions for 20 min in the first PVCL/PMAA adsorption cycle, then for 10 min from the second deposition cycle on. Each adsorption was followed by two rinsing steps (2 min each) with a 150 mM NaCl solution of same pH as used for polymer adsorption. To label NTs, PAH and PAH-Rh (0.5 mg/mL) was alternately deposited in PSS/PAH deposition cycles. Both sides of the membrane were decrusted with a cotton swab every second cycle during PVCL/PMAA

deposition and every fourth cycle during PSS/PAH deposition, to prevent nanopore blockage. When the desired number of bilayers was obtained, the membranes were decrusted, rinsed with MilliQ water and stored in a fridge.

When (ALG/CHI) was used instead of (PSS/PAH) to prepare bi-compartmentalized $(PVCL/PMAA)_{5.5}(ALG/CHI)_{12}$ NTs, the same procedure was followed, except that the membranes were decrusted every second cycle and that PAH-Rh was used to form two (ALG/PAH-Rh) bilayers during the fifth and sixth cycles of deposition in order to fluorescently-tag the NTs.

Collection of NTs at pH 6.5

A circular $(PVCL/PMAA)_{5.5}/(PSS/PAH)_{12}$ membrane (12 mm diameter) was placed in a Swinny filtration unit, and 120 mL of pH 6.5 buffer (20 mM MES and 150 mM NaCl) was pushed through the membrane (Scheme 1c) to disaggregate the $(PVCL/PMAA)_{5.5}$ external compartment and release the $(PSS/PAH)_{12}$ NTs which were collected in MES buffer. For microscopy observation, the released NTs were filtered onto a blank PC membrane covered with 20 nm of gold (for scanning electron microscopy), then rinsed three times with 4 mL MilliQ water to remove salt traces (Scheme 1c). $(ALG/CHI)_{12}$ NTs were released and collected in the same way by treating $(PVCL/PMAA)_{5.5}/(ALG/CHI)_{12}$ membrane with pH 6.5 MES/150 mM NaCl buffer.

After pH 6.5 MES treatment, the NTs remaining in the pores were also collected. For this purpose, the MES-treated LbL membrane was placed in 3 mL dichloromethane and shaken for 10 min to fully dissolve the PC template. The NTs were filtered onto a blank PET membrane (200 nm pore diameter) and rinsed three times (5 mL each) with fresh dichloromethane to remove PC traces.

Characterization of the thickness of flat LbL films

The thickness of dry LbL films was measured in air by spectroscopic ellipsometry (Jobin-Yvon UVisel) at an incidence angle of *ca.* 65˚, with wavelengths ranging from 400 to 700 nm. The refractive index of the dry film (including the *ca.* 1.5 nm of native silicon oxide thickness) was fixed to 1.50, and the refractive index of Si was taken from the literature.[39] To monitor the thickness change of the film in solution, we used spectroscopic *in-situ* ellipsometry at *ca.* 65° incidence angle and wavelengths varying from 400 to 700 nm. The film was placed in an Accurion temperature-controlled liquid cell (volume 0.7 mL) aligned on a home-made multi-axis sample stage. Then 20 mM MES buffer (20˚C) at a fixed pH and NaCl concentration was added into the cell and circulated at *ca.* 1 mL/min. The film thickness was obtained by fitting the data with a two-layer model, using the tabulated refractive index for Si and a fitted Cauchy transparent model for the film. The refractive index of water and its temperature-, wavelength-, and NaCl concentration-dependence were obtained from literature.[40,41]

Characterization of NTs

Measurement of the thickness of the compartments in pores. The thickness of $(PVCL/PMAA)_{m.5}$ and $(PSS/PAH)_n$ compartments deposited in the pores of PC membranes was determined by calculating the average pore diameter after gas flow porometry measurements performed before and after LbL assembly. For the measurement, a dry PC membrane was firmly held inside a membrane holder with an effective section area of 0.137 cm^2. Filtered air gas at room temperature was flown upstream with a pressure ranging from 0.35 to 4 bar. The gas flow rate (mL/min) downstream from the sample was measured with a calibrated GFM Pro Gas Flowmeter from Thermofisher Scientific. The inner diameter of the pores was calculated by using Knudsen diffusion and the Hagen-Posieuille flow relationship, as described

elsewhere.[42]

Morphology of NTs in membrane. The membranes filled with LbL NTs were coated by 20 nm of sputtered gold and their flat faces were imaged with a scanning electron microscope SEM (JSM-7600F, JEOL Ltd) at 5 kV. Non-coated membranes containing fluorescently-tagged NTs were additionally imaged by epifluorescence microscopy (red channel, Olympus IX71). Since this only provides images of the tips of the NTs, the filled membranes were embedded in paraffin[43] and microtomed, and 5 µm thick sections were imaged by a Zeiss LSM 710 confocal microscope.

Morphology of liberated NTs and trapped NTs. The NTs liberated under buffer treatment were collected over a gold-coated PC membrane, and observed by SEM (5 kV) and epifluorescence microscopy. The trapped NTs (*i.e.*, NTs which remained in the nanopores of PC membranes after buffer treatment were collected on a PET membrane after dissolution of the PC membrane template and observed directly by epifluorescence microscopy or SEM (in which case the samples were coated with 20 nm of gold).

Quantification of the amount of liberated NTs. The amount of rhodamine-labeled NTs liberated after buffer treatment was measured by fluorescence spectroscopy. The total amount of NTs was obtained by dissolving 0.5 cm^2 of filled membrane in 1 mL dichloromethane, and by measuring the fluorescence at 590 nm of the NTs suspension with a Varian Cary Eclipse fluorescence spectrophotometer (550 nm excitation wavelength). A blank was subtracted using as reference the same membrane filled with non-fluorescent NTs. The amount of NTs trapped in the membrane after disaggregation of the outer sacrificial compartment was measured similarly, by dissolving the membrane obtained after pH 6.5 treatment and expulsion of the trapped NTs. The proportion of NTs liberated from the membrane was obtained by comparing the

fluorescence intensity of the total number of NTs and the one of the trapped NTs.

Results and discussion

Effect of pH and salt concentration on the growth and disintegration of PMAA/PVCL LbL films

The lower critical solution temperature (LCST) of PVCL was previously shown to decrease in the presence of SO_4^{2-}, $H_2PO_4^-$ or Cl^- in aqueous solution, suggesting strong salt effects on the hydrophobicity of the chain.[44] Therefore, we monitored the growth and stability of $(PMAA/PVCL)_m$ films depending on ionic strength, having in mind biological applications for which a background NaCl concentration of 150 mM is typical. $(PMAA/PVCL)_m$ films were thus deposited on PEI-modified Si wafers at pH 2.0 in 0, 50 or 150 mM NaCl solutions, using a low molar mass PVCL (M_w 1.8 kg/mol). The dry thickness of PEI/$(PMAA/PVCL)_m$ films versus number of deposited bilayers is shown in Figure 1a. A linear growth is observed with an average thickness increment per bilayer of 4.1 nm and no significant influence of salt concentration on film growth, showing that PMAA/PVCL multilayers do not have a significant electrostatic contribution to stability at pH 2.0. This is in marked contrast compared to a weakly H-bonded LbL system such as PAA/PEO, whose film growth was reported to be completely inhibited in 500 mM NaCl.[45]

The stability of a thick PEI/$(PMAA/PVCL)_{20}$ film (starting dry thickness d_0 = 85 nm) was then assessed in solutions of increasing pH. The films were immersed in 20 mM MES buffer at a given pH for 1 min, rinsed with water to remove the adsorbed salt, dried, and their dry thickness (d) was measured again by ellipsometry. For all experiments, the stability of LbL multilayers was tested at the same NaCl concentration

as the one used for film growth. The relative film thickness, d/d_0, is plotted versus immersion pH in Figure 1b, from which the critical pH for disintegration, pH_{crit}, can be obtained as the pH corresponding to half-disintegration. The pH_{crit} of PEI/$(PMAA/PVCL)_{20}$ films decreased with the salt concentration, being 7.1, 6.6, and 6.1 for 0, 50, and 150 mM NaCl, respectively. Simultaneously, the disintegration curves were steeper at higher salt concentrations: for instance, at 150 mM NaCl, a 0.1 increment in pH units (from 6.0 to 6.1) resulted in the full disintegration in 1 min of the initially-stable film, whereas an increment of 0.5 pH units (from 7.0 to 7.5) was required to have the same effect in the absence of salt. The differences of steepness of the disintegration curves depending on salt content probably arise from the more homogeneous electrostatic environment existing at higher ionic. pH_{crit} is decreased and H-bonds are weakened in the presence of salts because of, *e.g.*, promotion of polymer ionization and change of polymer solubility and hydration.

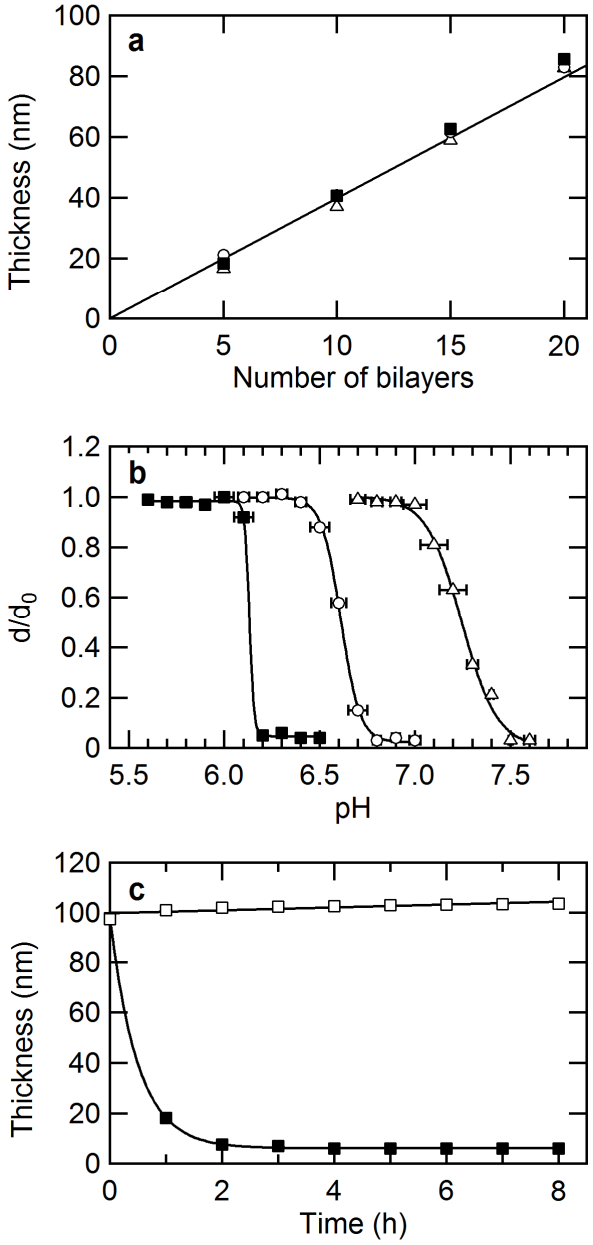

Figure 1. (a) Dry thickness of PEI/(PMAA/PVCL)$_m$ LbL films grown at pH 2.0, in 0 (triangles), 50 (circles), or 150 mM (squares) NaCl. The line is a fit to the data. (b) Relative dry thickness (d/d_0) of PEI/(PMAA/PVCL)$_{20}$ films (d_0 *ca.* 85 nm, corresponds to the initial dry thickness of the film) grown in 0 (triangles), 50 (circles), or 150 mM (squares) NaCl and subsequently immersed for 1 min in 20 mM MES buffers of different pH as indicated. The curves are sigmoidal fits. (c) *In-situ* measurements of the thickness of PEI/(PMAA/PVCL)$_{20}$ films initially grown in 150 mM NaCl at pH 2.0,

and subsequently immersed in 20 mM MES buffer (150 mM NaCl) at pH 5.7 (hollow squares) and 6.0 (filled squares). The MES buffer was flown at the constant rate of 1 mL/min during the measurements. The curves are drawn to guide the eye.

The long term stability of PEI/$(PMAA/PVCL)_{20}$ films was also studied at pH 5.7 and 6.0 (just below the pH_{crit} measured for a 1 min immersion time) in 20 mM MES (150 mM NaCl) buffer (Figure 1c). At pH 5.7, a PEI/$(PMAA/PVCL)_{20}$ film of 85 nm dry thickness swelled to 100 nm upon immersion; its thickness then remained essentially constant over the next 8 h, with only a very slight increase over time indicating limited reorganization. This film was then rinsed, dried, and its dry thickness was measured again by ellipsometry, providing a value of 86 nm, very close to its original dry thickness. At pH 6.0, the PEI/$(PMAA/PVCL)_{20}$ film also rapidly swelled to 100 nm when immersed in MES buffer; however, contrasting with the case of pH 5.7, the film slowly disaggregated with 80% of the film removed in 1 h and a complete disintegration in 2 h. This illustrates that the pH_{crit} is a time-dependent parameter and that the kinetics of film disaggregation vary substantially around pH_{crit}. When farther below pH_{crit} as at pH 5.7, the film is stable for extended periods of time.

Similar experiments were performed on the PMAA/PVPON LbL system, in which the H-bond acceptor component is of increased polarity compared to PVCL (Supporting Information). The pH_{crit} of these PMAA/PVPON multilayers was significantly lower than for the PMAA/PVCL system; in the sequel, we thus concentrate on PMAA/PVCL multilayers fabricated from 150 mM NaCl, since they meet our stability criteria for biological work.

Effect of PVCL molar mass on the growth and disintegration of PMAA/PVCL films

Previous studies have shown that polymer molar mass as well as the difference of molar mass between components in H-bonded multilayers can lead to different film thickness.[46] Weakly H-bonded LbL systems, such as PAA/PEO and PMAA/PEO, were especially shown to be very sensitive to PEO molar mass: when the PEO molar mass increased from 1.5 to 20 kg/mol, the film thickness increased by a factor of seven.[45] Additionally, one might expect that larger molar masses would be conducive to more stable multilayers, due to the increased number of H-bonds per chain. Therefore, films comprising PVCL of M_w 1.8, 32 and 240 kg/mol were grown in conditions identical to before (*i.e.*, pH 2.0 and 150 mM NaCl), and their stability was assessed versus pH. The average thickness increment per bilayer was 4.2 nm for the three types of PEI/(PMAA/PVCL)$_m$ films, independent of PVCL molar mass (Figure 2a). This molar mass independence again hints to strong H-bonds in the PMAA/PVCL system. Accordingly, when the stability of PEI/(PMAA/PVCL)$_{20}$ films deposited from PVCL of different molar masses was measured in solutions of increasing pH (Figure 2b), the pH_{crit} was found to be independent of molar mass (6.1, 6.1 and 6.2, for PVCL of M_w 1.8, 32 and 240 kg/mol, respectively).

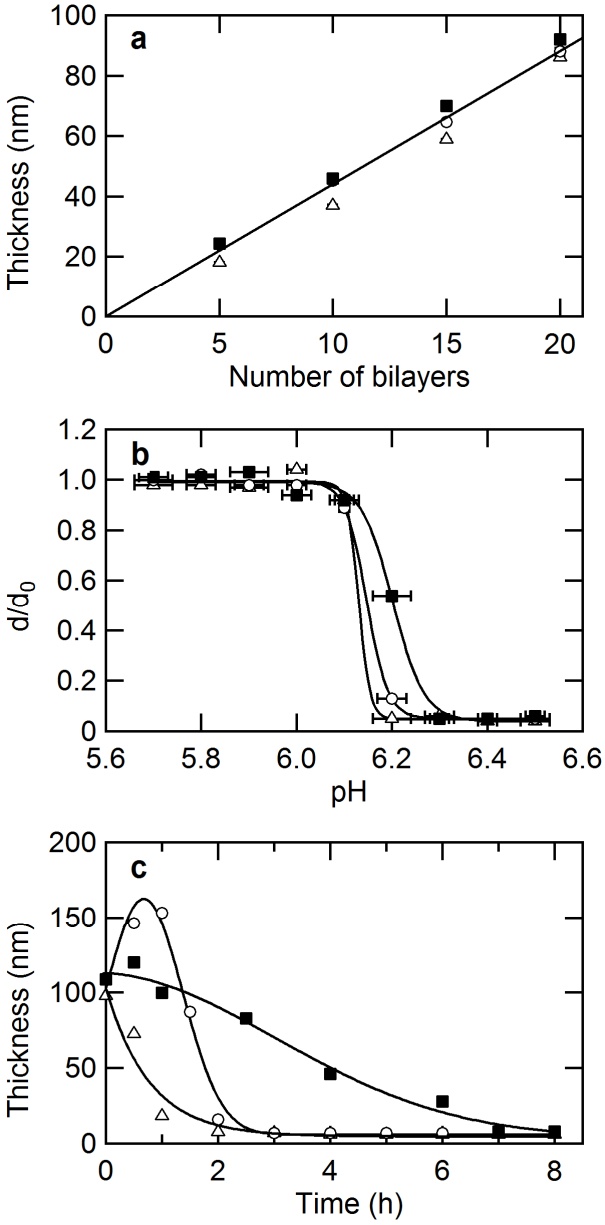

Figure 2. (a) Dry thickness of PEI/(PMAA/PVCL)$_m$ films comprising PVCL of different molar masses, grown at pH 2.0 in150 mM NaCl. The lines are fits to the data. (b) Relative dry thickness (d_0/d) of PEI/(PMAA/PVCL)$_{20}$ films grown at pH 2.0 then immersed in 20 mM MES buffer (150 mM NaCl) for 1 min. The curves are sigmoidal fits. (c) In-situ thickness of PEI/(PMAA/PVCL)$_{20}$ films initially grown in 150 mM NaCl at pH 2.0, and subsequently immersed in pH 6.0, 20 mM MES buffer (150 mM NaCl). The curves are drawn to guide the eye. Molar mass of PVCL: 1.8 (triangles), 32

(circles), or 240 kg/mol (squares).

The long term stability of these films was also measured at pH 6.0 (Figure 2c). The film comprising the low molar mass PVCL (M_w 1.8 kg/mol) directly swelled from 85 to 100 nm upon immersion in the MES buffer, and fully disaggregated in 2 h. In contrast, PEI/(PMAA/PVCL)$_{20}$ films comprising PVCL of higher molar mass swelled more slowly, then gradually disaggregated at a slower rate. The higher the molar mass of PVCL, the longer the time for full film disaggregation (3 and 7 h for 32 and 240 kg/mol, respectively). Hence, although the three films have a similar pH_{crit} when measured for short immersion times (1 min), their disaggregation kinetics depends on the molar mass of the PVCL component when probed at a pH just below the critical one, probably resulting from the molar mass dependence of disentanglement kinetics. By increasing the PVCL molar mass, a slight increase of dynamic stability can thus be obtained.

Summing up, PMAA/PVCL multilayers growth is independent of NaCl concentration and PVCL molar mass these H-bonded films can be disaggregated by a pH trigger, with pH_{crit} strongly depending on salt concentration and very weakly on PVCL molar mass. The transition between stable and unstable films occurs over a narrow range of pH values, with the critical pH being generally compatible with sensitive biological components. In the sequel, we thus concentrate on utilizing PMAA/PVCL multilayers as sacrificial compartments for the release of flat LbL films and of LbL NTs, essentially using the lower molar mass PVCL (1.8 kg/mol) and films grown in 150 mM NaCl unless otherwise indicated.

Use of $(PMAA/PVCL)_m$ as sacrificial compartment for the release of flat LbL films

$PEI/(PMAA/PVCL)_{20}(PSS/PAH)_n$ bi-compartmentalized films were prepared by the LbL deposition at pH 4.0 of $(PSS/PAH)_n$ films over a $PEI/(PMAA/PVCL)_{20}$ compartment of 85 nm dry thickness, initially grown at pH 2.0. As shown in Figure 3a, the thickness of the $(PSS/PAH)_n$ film was insensitive to whether it was grown over a PEI-coated Si wafer or over a $PEI/(PMAA/PVCL)_{20}$ compartment, with an average thickness increment per bilayer of 2.5 nm. The long term stability of this $PEI/(PMAA/PVCL)_{20}(PSS/PAH)_{20}$ film was then monitored at pH 6.0 in 20 mM MES buffer (150 mM NaCl) by in-situ ellipsometry. Single $PEI/(PMAA/PVCL)_{20}$ and $PEI/(PSS/PAH)_{20}$ films were also tested in the same conditions (Figure 3b). The single $PEI/(PMAA/PVCL)_{20}$ film fully disaggregated in 2 h, whereas the single $PEI/(PSS/PAH)_{20}$ compartment was stable at pH 6.0 for 8 h. In contrast, the bi-compartmentalized film immediately swelled from 125 nm (dry film total thickness) to 150 nm upon immersion, then gradually swelled to 200 nm and started to erode after 4 h, until the film fully detached after 8 h. Obviously, the upper pH-stable $(PSS/PAH)_{20}$ compartment acted as a barrier delaying but not preventing the disaggregation of the buried PMAA/PVCL compartment.

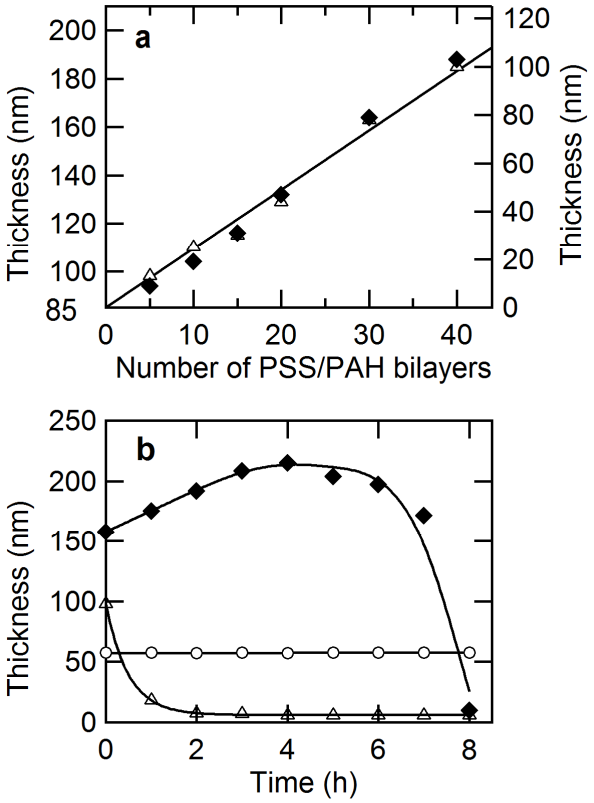

Figure 3. (a) Dry thickness of bi-compartmentalized PEI/(PMAA/PVCL)$_{20}$/(PSS/PAH)$_n$ films (squares, left axis) and of PEI/(PSS/PAH)$_n$ films (triangles, right axis) versus number of PSS/PAH bilayers. The (PSS/PAH)$_n$ films were deposited at pH 4.0 in 150 mM NaCl. The line is a fit to the data. (b) In-situ thickness of PEI/(PMAA/PVCL)$_{20}$/(PSS/PAH)$_{20}$ (squares), PEI/(PMAA/PVCL)$_{20}$ (triangles) and PEI/(PSS/PAH)$_{20}$ (circles) films immersed in pH 6.0, 20 mM MES buffer (150 mM NaCl). The MES buffer was flown at the constant rate of 1 mL/min during the measurements. The curves are drawn to guide the eye.

We then tested whether the upper (PSS/PAH)$_n$ films could be freely released from Si wafers by disaggregation of the underlying PMAA/PVCL compartments in such PEI/(PMAA/PVCL)$_m$/(PSS/PAH)$_n$ films. Three bi-compartmentalized films

comprising m = 5, 10, and 20 PMAA/PVCL bilayers were prepared, followed by n = 40 bilayers of PSS/PAH, with LbL deposition performed at pH 2.0 and 4.0 for $(PVCL/PMAA)_m$ and $(PSS/PAH)_{40}$ compartments, respectively. The floating-off of the $(PSS/PAH)_{40}$ films was tested at pH 6.5 in 20 mM MES buffer (150 mM NaCl). After immersion for 10 min, the films were fully released from the Si wafers for all the systems tested (Supporting information, Figure S2), but broke into several smaller pieces because of the low mechanical strength of $(PSS/PAH)_{40}$ films. The floating film fragments were collected on clean Si wafers, rinsed and dried to check their thickness, which was *ca.* 100 nm, corresponding to the initial dry thickness of the $(PSS/PAH)_{40}$ compartment. This demonstrates that H-bonded $(PMAA/PVCL)_m$ films are proper sacrificial compartments for the release of overgrown electrostatic LbL multilayers.

Use of $(PVCL/PMAA)_{m.5}$ as sacrificial compartment for the liberation of LbL NTs.

Encouraged by these results on flat films, we then evaluated the possibility to release by the same mechanism LbL NTs grown in templating track-etched nanoporous PC membranes. The growth of the sacrificial PVCL/PMAA compartment was first assessed in the pores of a PC membrane of 800 nm nominal pore diameter (750 nm measured pore diameter) with 4×10^7 pores cm^2 (Scheme 1b). The PVCL/PMAA growth was linear after two bilayers, with an average thickness increment per bilayer of 35 nm (Supporting information, Figure S3). This is much larger than the growth increment measured for flat multilayers (4.1 nm/bilayer, Figure 1a), which is typical for LbL assembly in nanopores as extensively reported before for electrostatic multilayers;[23,27,42,47-49] apparently, the same phenomena (crowding of chains leading to gel formation, bridging of chains between opposite pore walls, etc.) happen for H-bonded multilayers as well. Since this hints at a possible change of multilayer structure,

we checked that the disaggregation of the nano-confined $(PVCL/PMAA)_{m.5}$ multilayers was not hindered at physiological pH. A PC membrane filled with $(PVCL/PMAA)_{8.5}$ multilayers of 210 nm residual average dry pore diameter was thus immersed in 20 mM MES buffer (150 mM NaCl) at pH 6.5, rinsed, dried, and the pore diameter of the membrane was measured again by gas flow porometry. A value of 750 nm was found, which is identical to that of the starting unfilled PC membrane, indicating quantitative disintegration of the LbL NTs in the membrane.

Therefore, bi-compartmentalized $(PVCL/PMAA)_{5.5}/(PSS/PAH)_{12}$ NTs were grown in the same type of PC membrane, at pH 2.0 and 4.0 for $(PVCL/PMAA)_{5.5}$ and $(PSS/PAH)_{12}$ compartments, respectively. The thickness of the two compartments was 65-75 nm and 210-240 nm, respectively. Unfortunately, subsequent immersion of the bi-compartmentalized NTs-filled PC membrane in pH 6.5 MES buffer did not lead to any collection of NTs. We suspected that this resulted from the $(PSS/PAH)_{12}$ inner NTs compartment adhering on the nanopore walls after dissolution of the sacrificial compartment. Therefore, we used a forced expulsion process to release and collect the NTs (Scheme 1c). 120 mL of pH 6.5, 20 mM MES buffer (150 mM NaCl) was flown through the filled membrane to disaggregate the sacrificial compartment and expel the liberated $(PSS/PAH)_{12}$ inner NT compartment. The liberated NTs and trapped NTs were collected by filtration and imaged by microscopy (Figure 4a-d). The SEM image shows that the liberated NTs are *ca.* 24 µm long, which corresponds to pore length, and 1 µm wide, which is larger than the expected outer diameter of the $(PSS/PAH)_{12}$ compartment and is due to the swelling and flattening of the NTs during collection. This demonstrates the possibility to directly release NTs in bio-compatible aqueous solution without using organic solvent or dissolving the template. The NTs still trapped in the membrane after the treatment at pH 6.5 were also collected on a porous PET

membrane, by dissolving the PC membrane in dichloromethane (Figure 4c,d); these trapped NTs have the same size as liberated ones.

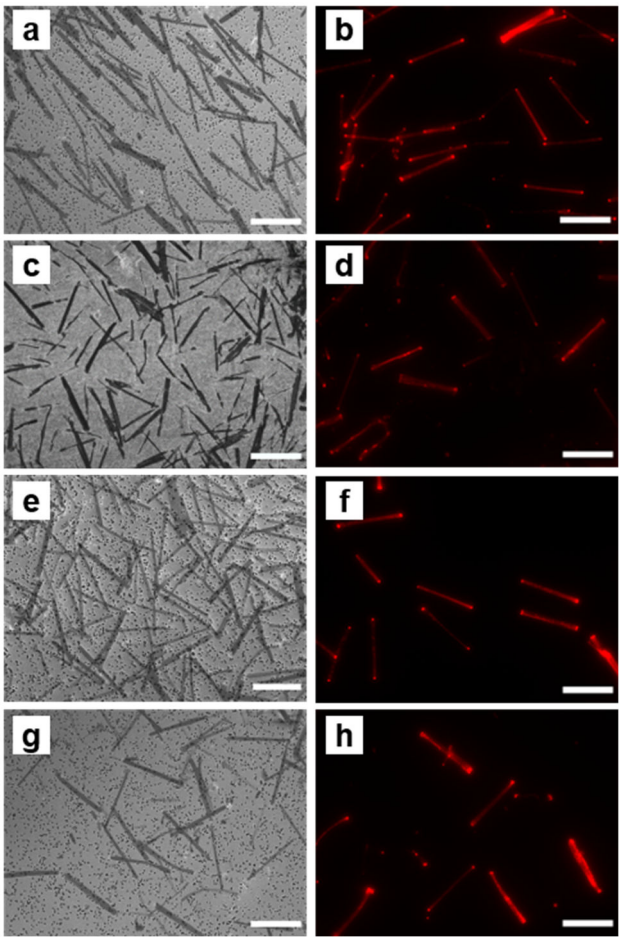

Figure 4. SEM (left column) and epifluorescence microscopy images (right column) of NTs. (a,b) Liberated $(PSS/PAH)_{12}$ NTs obtained by dissolving at pH 6.5 the sacrificial compartment of bi-compartmentalized $(PVCL/PMAA)_{5.5}/(PSS/PAH)_{12}$ NTs in membranes. (c,d) The remaining NTs trapped in the membrane after pH 6.5 treatment, recovered by dissolving the membrane in dichloromethane. (e,f) Same as (a,b), except for the molar mass of PVCL which was 240 kg/mol. (g,h) Liberated $(ALG/CHI)_{12}$ NTs obtained by dissolving at pH 6.5 the sacrificial compartment of bi-compartmentalized $(PVCL/PMAA)_{5.5}/(ALG/CHI)_{12}$ NTs in membranes. Scale bars: 20 µm.

The PC membranes were also observed by SEM, epifluorescence microscopy and confocal microscopy before and after the liberation of $(PSS/PAH)_{12}$ NTs (Figure 5). Although many pores were opened by the release process as shown in the SEM images (Figure 5c), a substantial amount of NTs was not liberated (Figure 5f). The 3D reconstruction of confocal microscopy images of microtomed membranes also demonstrates the partial liberation of NTs at pH 6.5 (Figure 5i). Since rhodamine-tagged PAH (PAH-Rh) was used to label NTs, the fluorescence of the collected suspensions of NTs can be used to quantify their amount. The fluorescence of PAH-Rh solutions of varying concentration was measured in pH 4.0/6.5 MES buffer (Supporting information, Figure S4), showing that the fluorescence intensity at 590 nm is proportional to PAH-Rh concentration regardless of the pH value. In order to quantify the fraction of liberated NTs, the fluorescence of suspensions containing all NTs or only trapped NTs was measured, by dissolving the initially filled membrane and the membrane after pH 6.5 treatment in dichloromethane, respectively. An average fraction of liberated NTs of 51±6% was thereby obtained (Supporting information, Figure S5a).

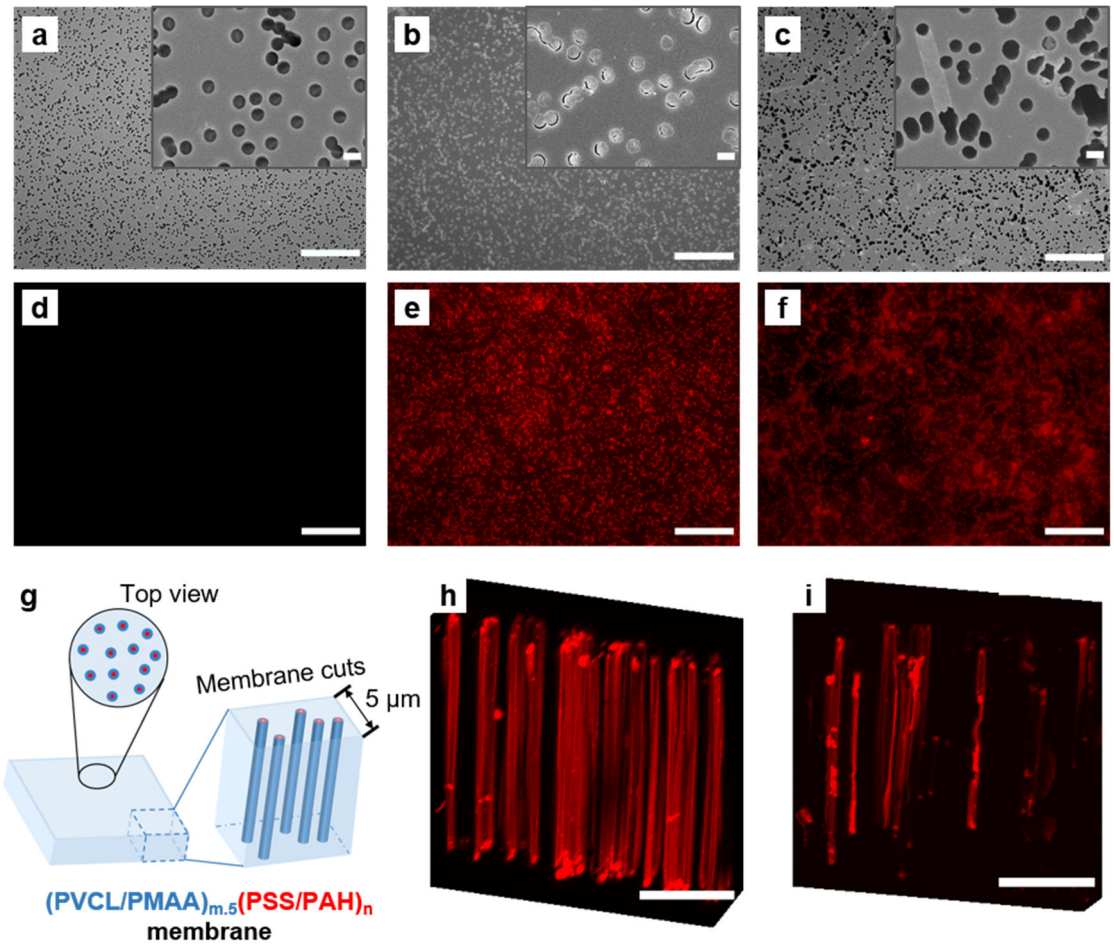

Figure 5. Microscopy images of (a,d) the virgin unfilled PC membrane, (b,e,h) a membrane filled with $(PVCL/PMAA)_{5.5}/(PSS/PAH)_{12}$ NTs, and (c,f,i) a membrane after the liberation of the NTs at pH 6.5. (a-c) Top-view SEM images; scale bars: 20 µm, scale bars of insets: 1 µm. (d-f) Top-view epifluorescence microscopy images; scale bars: 20 µm. (g,h,i) Scheme of the sample and tridimensional reconstruction of confocal microscopy images of microtomed membrane cuts (5 µm thickness); scale bars: 10 µm.

The reason why some NTs are not liberated is that overlapping pores in the membrane create fused NTs that are physically blocked in the membrane. According to the manufacturer, the proportion of overlapping pores is *ca.* 55%, close to the 49% of

membrane-trapped NTs found by fluorescence spectroscopy. In order to confirm this hypothesis, we performed a similar experiment on a PC membrane of four times lower pore density (1×10^7 pores cm^2), corresponding to a lower proportion of overlapped pores of 18% according to the manufacturer. The proportion of collected NTs logically increased to 83±5% (Supporting information, Figure S5b). Note that the trapping of fused NTs in the membranes can be seen as a positive outcome of our methodology, since it results in the exclusive collection of single NTs, contrarily to what happens when dissolving the membranes.

The effect of PVCL molar mass and (PVCL/PMAA) compartment thickness on the efficiency of the release process were also studied. Bi-compartmentalized $(PVCL/PMAA)_{5.5}/(PSS/PAH)_{12}$ NTs were prepared from 32 and 240 kg/mol PVCL and their inner $(PSS/PAH)_{12}$ NTs were liberated at pH 6.5 (Figure 4e,f). The released NT fraction was 60±11% and 55 ±13%, respectively, non-significantly different from the 51±6% obtained with 1.8 kg/mol PVCL. This is in agreement with the almost insignificant influence of PVCL molar mass on the critical pH of PVCL/PMAA flat films. The effect of the thickness of the sacrificial (PVCL/PMAA) compartment on tube release was also studied for a PC membrane of larger pore diameter (Supporting information, Figure S6). Although thicker sacrificial compartments resulted in a slightly higher fraction of liberated tubes, the amount of liberated tubes always remained close to the fraction of non-overlapping pores in the membrane.

Finally, in order to test the release of more biologically-compatible NTs, ALG/CHI LbL multilayers were deposited instead as PSS/PAH for the inner compartment. The measurement of the growth of ALG/CHI multilayers over a flat surface provided a thickness increment per bilayer of 2.7 nm, close to the 2.5 nm of the PSS/PAH system. The floating-off of the ALG/CHI film was also observed when immersing a flat

$(PVCL/PMAA)_{20}(ALG/CHI)_{40}$ film in pH 6.5 MES/NaCl buffer for 1 h. However, compared with PSS/PAH films, the higher swelling degree of CHI/ALG films (70% as measured by in-situ ellipsometry) resulted in a lower rigidity and mechanical strength which prevented to collect the film after floating-off. The liberation of $(ALG/CHI)_{12}$ NTs was then carried out on a $(PVCL/PMAA)_{5.5}(ALG/CHI)_{12}$-filled membrane according to the same procedure as for (PSS/PAH)-based NTs. Fluorescence spectroscopy provided a fraction of liberated $(ALG/CHI)_{12}$ NTs of 60±8%, close to what was obtained for (PSS/PAH)-based NTs. Additionally, the liberated $(ALG/CHI)_{12}$ NTs were intact and exhibited the expected morphology (Figure 4g,h). This demonstrates that our biocompatible liberation conditions can be applied to different types of systems, and are well-adapted for the production of polysaccharide nanotubes at close-to-neutral saline condition. It is therefore suited to the encapsulation of sensitive biological components such as enzymes or even living organisms.

Conclusions

Summing up, we have studied the growth and stability of H-bonded multilayers based on PMAA and PVCL. PMAA/PVCL multilayer growth at low pH was independent of NaCl concentration and PVCL molar mass, due to strong H-bonding between this pair of polymers. The disaggregation of the films was then performed at higher pH values. The critical pH for disaggregation was found to depend strongly on salt concentration, whereas PVCL molar mass did not play an important role. Interestingly, the PVCL/PMAA system is compatible with biologically-sensitive components, as it provides multilayers which are stable just below pH 6.0 and can be disaggregated in 0.15 M NaCl neutral pH conditions.

We then demonstrated the liberation of flat PSS/PAH films by disaggregating a sacrificial PMAA/PVCL compartment, and implemented the methodology to the liberation of PSS/PAH NTs grown in templating PC membranes, then to the liberation of bio-compatible ALG/CHI NTs. We showed for the first time the possibility to liberate such tubes without having to dissolve the membrane, a methodology that could easily be generalized to other types of templating methods. The liberated NTs were directly obtained in benign conditions (pH 6.5, 150 mM NaCl) that are fully bio-compatible and promising for biological applications. The liberation process was close to quantitative with respect to the liberation of non-crossing NTs, and offers the supplementary advantage to eliminate crossing NTs from the collection process. We are now exploring the use of such nano- or micro-tubes for the fabrication of hybrid systems comprising biological cells.

ASSOCIATED CONTENT

Supporting Information

The following supplementary information is available free of charge: experiments performed on the (PMAA/PVPON) system, images of floated-off flat $(PSS/PAH)_{40}$ films, complementary experimental data on the growth of PVCL/PMAA multilayers in 800 nm PC membranes, fluorescence calibration of PAH-Rh at pH 4.0 and 6.5, quantification by fluorescence spectroscopy of the amount of released NTs, and the effect of the number of sacrificial bilayers on the fraction of released NTs.

AUTHOR INFORMATION

Corresponding Authors

*Email: alain.jonas@uclouvain.be

Author Contributions

The manuscript was written through contributions of all authors. All authors have given approval to the final version of the manuscript.

Notes

The authors declare no competing financial interest.

ACKNOWLEDGMENTS

The authors thank it4ip (Belgium) for track-etched PC and PET membranes, Laurent Jonckheere for gas flow porometry measurements, Pascale Lipnik for microtomy, Delphine Magnin for SEM, Marie-Christine Eloy for confocal microscopy, and Simon Cerfontaine for fluorescence spectroscopy. W.X. thanks the China Scholarship Council (CSC) and Université catholique de Louvain for a research fellowship. K.G. is a Research Associate of the F.R.S.-FNRS. The work was supported by the F.R.S.-FNRS.

References

(1) Yan, Y.,Björnmalm, M.; Caruso, F. Assembly of Layer-by-Layer Particles and Their Interactions with Biological Systems. *Chem. Mater.* **2013**, *26*, 452-460.
(2) Lee, S.,Yeom, B.,Kim, Y.; Cho, J. Layer-by-Layer Assembly for Ultrathin Energy-Harvesting Films: Piezoelectric and Triboelectric Nanocomposite Films. *Nano Energy* **2019**, *56*, 1-15.
(3) Koklukaya, O.,Carosio, F.,Grunlan, J. C.; Wagberg, L. Flame-Retardant Paper from Wood Fibers Functionalized via Layer-by-Layer Assembly. *ACS Appl. Mater. Interfaces* **2015**, *7*, 23750-23759.
(4) Ariga, K.,Yamauchi, Y.,Rydzek, G.,Ji, Q.,Yonamine, Y.,Wu, K. C.-W.; Hill, J. P. Layer-by-Layer Nanoarchitectonics: Invention, Innovation, and Evolution. *Chem. Lett.* **2013**, *43*, 36-68.
(5) Zhao, Y.,Zhang, Z.,Shi, L.,Zhang, F.,Li, S.; Zeng, R. Corrosion Resistance of a Self-Healing Multilayer Film Based on SiO_2 and CeO_2 Nanoparticles Layer-by-Layer Assembly on Mg Alloys. *Mater. Lett.* **2019**, *237*, 14-18.
(6) Wang, Y.,Angelatos, A. S.; Caruso, F. Template Synthesis of Nanostructured Materials via Layer-by-Layer Assembly. *Chem. Mater.* **2007**, *20*, 848-858.
(7) Fakhrullin, R. F.; Lvov, Y. M. "Face-Lifting" and "Make-Up" for Microorganisms: Layer-by-Layer Polyelectrolyte Nanocoating. *ACS Nano* **2012**, *6*, 4557-4564.
(8) Jeon, J.-W.,O'Neal, J.,Shao, L.; Lutkenhaus, J. L. Charge Storage in Polymer Acid-Doped Polyaniline-Based Layer-by-Layer Electrodes. *ACS Appl. Mater. Interfaces* **2013**, *5*, 10127-10136.
(9) Schlenoff, J. B. Retrospective on the Future of Polyelectrolyte Multilayers. *Langmuir* **2009**, *25*, 14007-14010.
(10) Boulmedais, F.,Tang, C. S.,Keller, B.; Vörös, J. Controlled Electrodissolution of Polyelectrolyte Multilayers: A Platform Technology Towards the Surface-Initiated Delivery of Drugs. *Adv. Funct. Mater.* **2006**, *16*, 63-70.
(11) Séon, L.,Lavalle, P.,Schaaf, P.; Boulmedais, F. Polyelectrolyte Multilayers: A Versatile Tool for Preparing Antimicrobial Coatings. *Langmuir* **2015**, *31*, 12856-12872.
(12) Cepak, V. M.; Martin, C. R. Preparation of Polymeric Micro-and Nanostructures Using a Template-Based Deposition Method. *Chem. Mater.* **1999**, *11*, 1363-1367.
(13) Azzaroni, O.; Lau, K. A. Layer-by-Layer Assemblies in Nanoporous Templates: Nano-Organized Design and Applications of Soft Nanotechnology. *Soft Matter* **2011**, *7*, 8709-8724.
(14) Kim, D. H.,Karan, P.,Göring, P.,Leclaire, J.,Caminade, A. M.,Majoral, J. P.,Gösele, U.,Steinhart, M.; Knoll, W. Formation of Dendrimer Nanotubes by Layer-by-Layer Deposition. *Small* **2005**, *1*, 99-102.
(15) Liang, Z.,Susha, A. S.,Yu, A.; Caruso, F. Nanotubes Prepared by Layer-by-Layer Coating of Porous Membrane Templates. *Adv. Mater.* **2003**, *15*, 1849-1853.
(16) Zhang, L.,Vidyasagar, A.; Lutkenhaus, J. L. Fabrication and Thermal Analysis of Layer-by-Layer Micro-and Nanotubes. *Curr. Opin. Colloid Interface Sci.* **2012**, *17*, 114-121.
(17) Komatsu, T.,Qu, X.,Ihara, H.,Fujihara, M.,Azuma, H.; Ikeda, H. Virus Trap in Human Serum Albumin Nanotube. *J. Am. Chem. Soc.* **2011**, *133*, 3246-3248.
(18) Hou, S.,Harrell, C. C.,Trofin, L.,Kohli, P.; Martin, C. R. Layer-by-Layer Nanotube Template Synthesis. *J. Am. Chem. Soc.* **2004**, *126*, 5674-5675.
(19) Lee, D.,Cohen, R. E.; Rubner, M. F. Heterostructured Magnetic Nanotubes. *Langmuir* **2007**, *23*, 123-129.
(20) He, Q.,Tian, Y.,Cui, Y.,Möhwald, H.; Li, J. Layer-by-Layer Assembly of Magnetic Polypeptide Nanotubes as a DNA Carrier. *J. Mater. Chem.* **2008**, *18*, 748-754.
(21) Shiraishi, Y.,Akiyama, M.,Sato, T.,Hattori, M.; Komatsu, T. Size-Dependent Dextran Loading in Protein Nanotube with an Interior Wall of Concanavalin A. *Polym. Adv. Technol.* **2014**, *25*, 1247-1251.
(22) Komatsu, T. Protein-Based Nanotubes for Biomedical Applications. *Nanoscale* **2012**, *4*, 1910-1918.

(23) Zhang, S.,Demoustier-Champagne, S.; Jonas, A. M. Quantitative Collection and Enzymatic Activity of Glucose Oxidase Nanotubes Fabricated by Templated Layer-by-Layer Assembly. *Biomacromolecules* **2015**, *16*, 2382-2393.
(24) Saghazadeh, S.,Zhang, S.,Lefèvre, D.,Le Beulze, A.,Jonas, A. M.; Demoustier-Champagne, S. Universal Method to Transfer Membrane-Templated Nano-Objects to Aqueous Solutions. *Langmuir* **2015**, *31*, 7264-7273.
(25) Yu, A.,Liang, Z.; Caruso, F. Enzyme Multilayer-Modified Porous Membranes as Biocatalysts. *Chem. Mater.* **2005**, *17*, 171-175.
(26) Guedidi, S.,Yurekli, Y.,Deratani, A.,Déjardin, P.,Innocent, C.,Altinkaya, S. A.,Roudesli, S.; Yemenicioglu, A. Effect of Enzyme Location on Activity and Stability of Trypsin and Urease Immobilized on Porous Membranes by Using Layer-by-Layer Self-Assembly of Polyelectrolyte. *J. Membr. Sci.* **2010**, *365*, 59-67.
(27) Glinel, K.,Behrens, A.,Langer, R. S.,Jaklenec, A.; Jonas, A. M. Nanofibrillar Patches of Commensal Skin Bacteria. *Biomacromolecules* **2018**, *20*, 102-108.
(28) Ramírez-Wong, D. G.,Saghazadeh, S.,Van Herck, S.,De Geest, B. G.,Jonas, A. M.; Demoustier-Champagne, S. Uptake of Long Protein-Polyelectrolyte Nanotubes by Dendritic Cells. *Biomacromolecules* **2017**, *18*, 4299-4306.
(29) Kharlampieva, E.,Kozlovskaya, V.; Sukhishvili, S. A. Layer-by-Layer Hydrogen-Bonded Polymer Films: From Fundamentals to Applications. *Adv. Mater.* **2009**, *21*, 3053-3065.
(30) Kharlampieva, E.; Sukhishvili, S. A. Hydrogen-Bonded Layer-by-Layer Polymer Films. *J. Macromol. Sci, Part C: Polym. Rev.* **2006**, *46*, 377-395.
(31) Lin, W.,Guan, Y.,Zhang, Y.,Xu, J.; Zhu, X. Salt-Induced Erosion of Hydrogen-Bonded Layer-by-Layer Assembled Films. *Soft Matter* **2009**, *5*, 860-867.
(32) Quinn, J. F.,Johnston, A. P.,Such, G. K.,Zelikin, A. N.; Caruso, F. Next Generation, Sequentially Assembled Ultrathin Films: Beyond Electrostatics. *Chem. Soc. Rev.* **2007**, *36*, 707-718.
(33) Yang, S.,Zhang, Y.,Zhang, X.; Xu, J. The Influence of pH on a Hydrogen-Bonded Assembly Film. *Soft Matter* **2007**, *3*, 463-469.
(34) Kozlovskaya, V.,Kharlampieva, E.; Sukhishvili, S. A., Hydrogen Bonded Layer-by-Layer Polymer Films and Capsules. Hydrogen-Bonded Interpolymer Complexes: Formation, Structure and Applications, 1st ed.; Khutoryanskiy, V. V.; Staikos, G., Eds. World Scientific: 2009; Vol. 12, pp 323-362.
(35) O'Neal, J. T.,Bolen, M. J.,Dai, E. Y.; Lutkenhaus, J. L. Hydrogen-Bonded Polymer Nanocomposites Containing Discrete Layers of Gold Nanoparticles. *J. Colloid Interface Sci.* **2017**, *485*, 260-268.
(36) Erel-Unal, I.; Sukhishvili, S. A. Hydrogen-Bonded Hybrid Multilayers: Film Architecture Controls Release of Macromolecules. *Macromolecules* **2008**, *41*, 8737-8744.
(37) Zhuk, A.,Pavlukhina, S.; Sukhishvili, S. A. Hydrogen-Bonded Layer-by-Layer Temperature-Triggered Release Films. *Langmuir* **2009**, *25*, 14025-14029.
(38) Erel-Unal, I.; Sukhishvili, S. A. Hydrogen-Bonded Multilayers of a Neutral Polymer and a Polyphenol. *Macromolecules* **2008**, *41*, 3962-3970.
(39) Palik, E. D., *Handbook of Optical Constants of Solids*. Academic press, INC: London, 1998; Vol. 1, p 564-565.
(40) Bashkatov, A. N.; Genina, E. A. Water Refractive Index in Dependence on Temperature and Wavelength: A Simple Approximation. *Proc. SPIE* **2003**, 393-396.
(41) Li, X.,Liu, L.,Zhao, J.; Tan, J. Optical Properties of Sodium Chloride Solution within the Spectral Range from 300 to 2500 nm at Room Temperature. *Appl. Spectrosc.* **2015**, *69*, 635-640.
(42) Roy, C.,Dupont-Gillain, C.,Demoustier-Champagne, S.,Jonas, A. M.; Landoulsi, J. Growth Mechanism of Confined Polyelectrolyte Multilayers in Nanoporous Templates. *Langmuir* **2009**, *26*, 3350-3355.
(43) Kappings, V.,Grün, C.,Ivannikov, D.,Hebeiss, I.,Kattge, S.,Wendland, I.,Rapp, B. E.,Hettel, M.,Deutschmann, O.; Schepers, U. vasQchip: A Novel Microfluidic, Artificial

Blood Vessel Scaffold for Vascularized 3D Tissues. *Adv Mater Technol-US* **2018**, *3*, 1700246.
(44) Zavgorodnya, O.,Kozlovskaya, V.,Liang, X.,Kothalawala, N.,Catledge, S. A.,Dass, A.; Kharlampieva, E. Temperature-Responsive Properties of Poly(N-vinylcaprolactam) Multilayer Hydrogels in the Presence of Hofmeister Anions. *Mater. Res. Express* **2014**, *1*, 035039.
(45) DeLongchamp, D. M.; Hammond, P. T. Highly Ion Conductive Poly(ethylene oxide)-Based Solid Polymer Electrolytes from Hydrogen Bonding Layer-by-Layer Assembly. *Langmuir* **2004**, *20*, 5403-5411.
(46) Su, C.,Sun, J.,Zhang, X.,Shen, D.; Yang, S. Hydrogen-Bonded Polymer Complex Thin Film of Poly(2-oxazoline) and Poly(acrylic acid). *Polymers* **2017**, *9*, 363.
(47) Alem, H.,Blondeau, F.,Glinel, K.,Demoustier-Champagne, S.; Jonas, A. M. Layer-by-Layer Assembly of Polyelectrolytes in Nanopores. *Macromolecules* **2007**, *40*, 3366-3372.
(48) Zhang, S.,Vlémincq, C.,Wong, D. R.,Magnin, D.,Glinel, K.,Demoustier-Champagne, S.; Jonas, A. M. Nanopapers of Layer-by-Layer Nanotubes. *J. Mater. Chem. B* **2016**, *4*, 7651-7661.
(49) Roy, C.,Buron, C.,Demoustier-Champagne, S.; Jonas, A. M., Nanoconfined Polyelectrolyte Multilayers: From Nanostripes to Multisegmented Functional Nanotubes. Multilayer Thin Films : Sequential Assembly of Nanocomposite Materials, 2nd ed.; Decher, G.; Schlenoff, J. B., Eds. Wiley-VCH Verlag & Co: Weinheim, Germany, 2012; Vol. 25, pp 613-636.